

Thermal Activation of the High Explosive NTO: Sublimation, Decomposition, and Autocatalysis

Gregory T. Long, Brittany A. Brems, and Charles A. Wight*

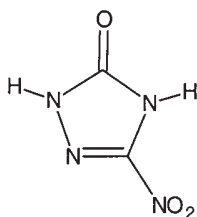
Center for Thermal Analysis, Department of Chemistry, University of Utah, Salt Lake City, Utah 84112

Received: July 26, 2001; In Final Form: January 15, 2002

Thermogravimetric analysis (TGA) and differential scanning calorimetry (DSC) show that the heating of 5-nitro-2,4-dihydro-3H-1,2,4-triazol-3-one (NTO) leads to competitive sublimation and condensed-phase exothermic decomposition. Model-free isoconversional analysis has determined activation energies (E_α) for these processes as a function of the extent of conversion, α . Sublimation occurs most readily in an open pan; although more than simple sublimation was observed, a global activation energy of $E_\alpha = 130\text{--}140\text{ kJ mol}^{-1}$ for sublimation was determined. Nonisothermal TGA and DSC traces run on pierced pan samples provide convincing evidence for competitive sublimation and condensed-phase decomposition of NTO. Confining NTO samples in a closed pan results in condensed-phase decomposition that leads to the formation of gaseous reaction products and shows autocatalytic behavior during the latter stages. Isoconversional analysis of DSC traces of closed pan samples yield activation energies for exothermic decomposition that increase from $E_\alpha = 273\text{ kJ mol}^{-1}$ for $\alpha = 0.01$ to a plateau of 333 kJ mol^{-1} for $0.17 \leq \alpha \leq 0.35$ prior to decreasing to 184 kJ mol^{-1} for $\alpha = 0.99$. The decrease in E_α with α during the latter stages of decomposition agrees with previous reports of autocatalytic behavior.

Introduction

5-Nitro-2,4-dihydro-3H-1,2,4-triazol-3-one (NTO) has shown considerable promise as an explosive; it has performance



characteristics similar to those of the widely used nitramine explosives hexahydro-1,3,5-trinitro-1,3,5-triazine (RDX) and octahydro-1,3,5,7-tetranitro-1,3,5,7-tetrazocine (HMX), but it is considerably less sensitive to accidental ignition by heat, impact, or spark.^{1,2}

One important aspect of the characterization of NTO includes the measurement of the kinetics and the associated Arrhenius parameters of its thermal decomposition. These parameters have been determined by various methods that include IR spectroscopy,³ thermogravimetric analysis (TGA),³ differential thermal analysis (DTA),⁴ differential scanning calorimetry (DSC),^{5,6} NO chemiluminescence,⁷ HPLC^{8,9} and GC¹⁰ analysis of partial decomposition in sealed capillaries, and T-jump/FTIR spectroscopy.¹¹ Williams and Brill (WB) have compiled and reevaluated kinetic data for the thermal decomposition of NTO; the reported activation energies (E_A) are in the range $170\text{--}504\text{ kJ mol}^{-1}$.¹¹ These workers have previously shown a linear correlation between $\ln A$ and E_A , which they refer to as a “kinetic compensation effect” and which may, in part, account for the wide range of reported activation energies.¹² They assert that

two processes dominate the global kinetics of the heating of NTO: sublimation and thermal decomposition.¹¹ Using isothermal and nonisothermal TGA, a range of values of $E_A = 108\text{--}130\text{ kJ mol}^{-1}$ and $\ln A = 29.2\text{--}31.1\text{ s}^{-1}$ were reported for the sublimation of NTO.¹¹ Reevaluation of kinetic data from several reports on the Arrhenius parameters for NTO led WB to recommend the use of values of $E_A = 326\text{--}364\text{ kJ mol}^{-1}$ and $\ln A = 67\text{--}78\text{ s}^{-1}$ for its thermal decomposition.¹¹

However, several studies have reported autocatalytic behavior during the latter stages of NTO thermal decomposition.^{3,8,10,13,14} Thus, no single value of the activation energy can adequately describe the entire decomposition. In fact, E_A would be expected to decrease during autocatalysis. More generally, activation energies often change during the course of a reaction in the solid state where multiple competing physical (polymorphic transition, diffusion, sublimation, adsorption, and desorption) and chemical (solid-state decomposition, product reactions with the solid, and gas-phase reactions) processes can occur simultaneously.¹⁵ Hence, a more accurate means of characterization of solid-state processes would employ a method that yields activation energies as a function of the extent of reaction, specified as E_α .

Model-free isoconversional analysis provides just such a method for studying solid-state reactions.^{15,16} Not only does isoconversional analysis give values of E_α versus α , it also avoids using a particular model in the analysis. To solve the commonly used rate expression for a solid-state reaction^{15–18} given in eq 1,

$$d\alpha/dt = k(T)f(\alpha) = Ae^{-E_\alpha/RT}f(\alpha) \quad (1)$$

a specific model must be used. Here, α is the extent of conversion, $f(\alpha)$ is the reaction model, $k(T)$ is a temperature-dependent rate constant, A is the Arrhenius preexponential factor, E_α is the activation energy, and R is the gas constant. Model-

* To whom correspondence should be addressed. E-mail: wight@chem.utah.edu.

dependent analysis results in model-dependent interpretations, which are rendered meaningless if the wrong model is chosen. To obtain a better understanding of solid-state processes, a model-independent method of analysis, such as isoconversional analysis, should be used. The isoconversional method has been successfully applied to the study of several energetic materials that include ammonium perchlorate (AP),¹⁹ ammonium nitrate (AN),²⁰ ammonium dinitramide (ADN),^{15,21,22} HMX,²³ and RDX.²⁴

The current study applies nonisothermal TGA and DSC to obtain decomposition kinetics and isoconversional analysis to determine activation energies as a function of α over the entire reaction. Sublimation is favored in open pans, and isoconversional analysis of TGA and DSC traces gives activation energies that are consistent with WB's recommended values for sublimation. Decomposition dominates in more confined environments, and isoconversional analysis of closed pan DSC traces shows a plateau region early in the decomposition that agrees with WB's recommended values for decomposition. Nonetheless, since the thermal decomposition of NTO is autocatalytic, it cannot be adequately described by a single activation energy as ascribed by WB. However, by determining the functional dependence of E_α on α using isoconversional analysis, both regions of the decomposition have been quantified. Thus, unlike any previous report, the present study yields a more complete understanding of the thermal stability of NTO by quantifying each event in its heating: sublimation, decomposition, and autocatalysis.

Experimental Section

Sample Preparation. NTO was synthesized¹ from the condensation reaction of formic acid and semicarbazide hydrochloride. The triazalone product was collected as a dry powder by overnight evaporation and was nitrated with 90% concentrated nitric acid. The resulting product was purified with three boiling aqueous recrystallizations and dried in air and had a melting point of 262 °C.

TGA Methods/Techniques. A Mettler-Toledo TGA/SDTA851^e module was used to perform TGA experiments in the nonisothermal heating mode for the temperature range 25–300 °C. Open pan experiments in 40 μ L Al pans used \sim 1.0 mg samples at linear heating rates of $\beta = 1.0, 2.5, 5.0, 7.5, 10.0, 12.5,$ and 15.0 °C min^{-1} . Pierced pan experiments used \sim 0.25 mg samples in 40 μ L Al pans at linear heating rates of $\beta = 2.5, 5.0, 7.5, 10.0,$ and 12.5 °C min^{-1} . N_2 was used as the carrier gas and flowed at a rate of 70 mL min^{-1} .

DSC Methods/Techniques. A Mettler-Toledo DSC821^e module was employed to collect DSC curves with nonisothermal heating programs over a temperature range of 25–300 °C. Al pans of 40 μ L volume were used in open pan, pierced pan, and closed pan experiments. In all DSC traces, positive going features correspond to exothermic processes and negative going features represent endothermic processes. The N_2 carrier gas flowed at a rate of 80 mL min^{-1} . In open pans, sample sizes of \sim 1.0 mg were used in experiments performed at heating rates of $\beta = 1.0, 2.5, 5.0, 7.5, 10.0, 12.5,$ and 15.0 °C min^{-1} . In pierced pan experiments, a 1.0 mm piercer was used to puncture pans lidded with crimp-sealed Al piercing lids that contained \sim 0.25 mg samples. The pierced pan experiments to determine the heat release as a function of β used sample sizes of \sim 1.0 mg. Experiments in pierced pans were performed at heating rates of $\beta = 2.5, 5.0, 7.5, 10.0, 12.5,$ and 15.0 °C min^{-1} . Closed pan experiments used pans lidded with crimp-sealed standard Al lids sealed under N_2 and were performed at heating rates of $\beta = 1.0, 2.5, 5.0, 7.5, 10.0, 12.5,$ and 15.0 °C min^{-1} . Sufficiently small samples were used (25–125 μ g) to prevent pan rupture.

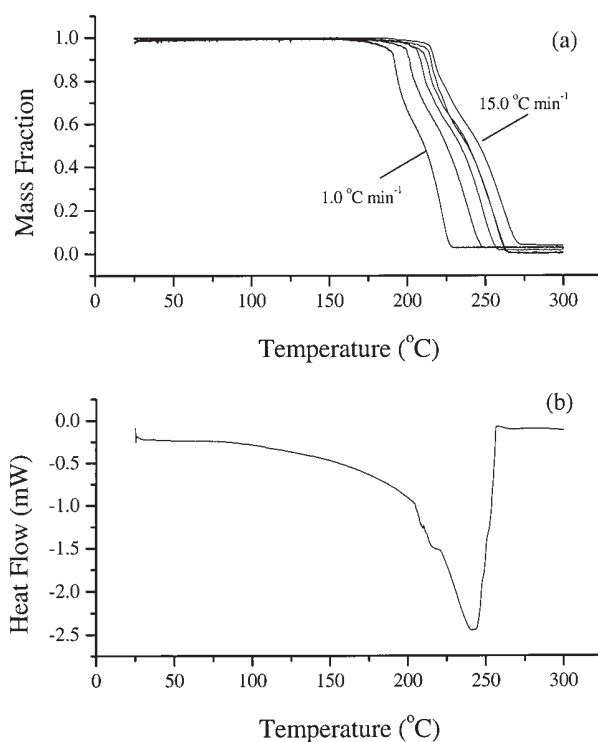


Figure 1. (a) Open pan nonisothermal TGA curves of NTO collected at constant heating rates of $\beta = 1.0, 2.5, 5.0, 7.5, 10.0, 12.5,$ and 15.0 °C min^{-1} . (b) A nonisothermal DSC trace collected for an open pan NTO sample at $\beta = 5.0$ °C min^{-1} .

Error Limits. Error limits shown in E_α versus α plots²⁰ and for the heat release, Q , represent 95% confidence limits.

Kinetic Analysis

Using the differential rate expression of a solid-state reaction given in eq 1, the model-free isoconversional method of analysis assumes that $f(\alpha)$ is independent of the temperature and the heating rate.^{15,16} A competition is set up between the temperature and the reaction rate in isothermal experiments and between the heating rate and the reaction rate in nonisothermal experiments. Equation 1 is integrated, and activation energies are determined from the relative mass loss in TGA traces and from the fractional peak areas in DSC traces at a particular extent of reaction. This procedure is repeated for different values of α to construct the functional dependence of E_α on α . The detailed procedure can be found in refs 20, 25, and 26.

Results

Open Pan Samples. A nonisothermal DSC trace acquired at a heating rate of 5.0 °C min^{-1} shows a broad endotherm below its melting point which occurs over a temperature range of 85–260 °C (Figure 1b). Analogous nonisothermal TGA experiments on open pan samples show a multistage mass loss that approaches 100% of the initial mass (Figure 1a). For $\beta = 5.0$ °C min^{-1} , the mass loss occurs over temperatures of 170–230 °C. Isoconversional analysis of the TGA traces leads to an E_α versus α plot that shows an initial increase from 140 to 260 kJ mol^{-1} and a decrease back to 155 kJ mol^{-1} for $0 < \alpha < 0.1$. After this stage, E_α shows a gradual and shallow decrease from 155 to 115 kJ mol^{-1} for $0.1 < \alpha < 1.0$ (Figure 2a). Similar analysis of open pan DSC traces results in an E_α versus α plot that increases from a value of 50 kJ mol^{-1} at $\alpha = 0.01$ to 115

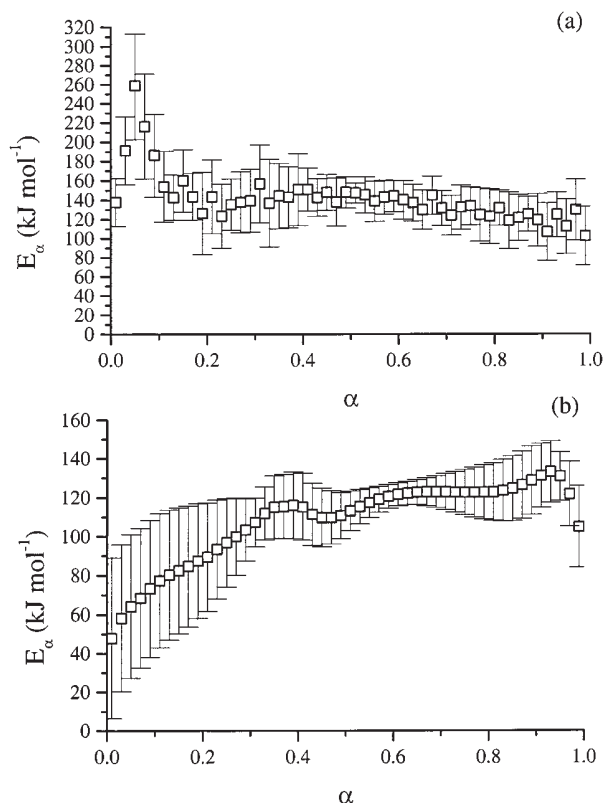


Figure 2. (a) An E_{α} versus α plot generated by applying isoconversional analysis to open pan TGA traces acquired at $\beta = 1.0, 2.5, 5.0, 7.5, 10.0, 12.5,$ and 15.0 °C min^{-1} . (b) An analogous E_{α} versus α plot as in (a) using open pan DSC traces acquired at $\beta = 1.0, 2.5, 5.0, 7.5, 10.0, 12.5,$ and 15.0 °C min^{-1} .

kJ mol^{-1} at $\alpha = 0.33$. From this point, E_{α} further increases with a very small gradient up to 130 kJ mol^{-1} for $\alpha = 0.95$ (Figure 2b).

Pierced Pan Samples. Nonisothermal TGA experiments for pierced pan NTO samples display a single-stage mass loss that occurs over a temperature range of $215\text{--}280$ °C (Figure 3a). This mass loss corresponds to only 78% of the initial mass. Nonisothermal DSC experiments for pierced pan samples exhibit significant changes as a function of heating rate (Figure 3b). For $\beta = 2.5$ °C min^{-1} , only a broad endotherm is observed. However, at a heating rate of 5.0 °C min^{-1} , a small exotherm succeeds the endotherm. Traces collected at $\beta = 7.5$ and 12.5 °C min^{-1} show that the size of the exotherm increases with increasing heating rate. The heat release increases as a function of heating rate in pierced pan experiments and approaches an asymptotic value of $Q = 1300 \text{ J g}^{-1}$ (169 kJ mol^{-1}), the value observed for closed pan samples (vide infra). Differences in the initial slopes are most likely due to small differences between the masses (and associated heat capacities) of the sample and reference pans.

Closed Pan Samples. The nonisothermal DSC trace in Figure 4a collected at 5.0 °C min^{-1} shows only an exotherm that appears between 255 and 270 °C. Isoconversional analysis of this exotherm results in an E_{α} versus α plot that increases from $E_{\alpha} = 273 \text{ kJ mol}^{-1}$ at $\alpha = 0.01$ to a plateau of $E_{\alpha} = 333 \text{ kJ mol}^{-1}$ for $0.17 \leq \alpha \leq 0.35$ prior to decreasing to $E_{\alpha} = 184 \text{ kJ mol}^{-1}$ at $\alpha = 0.99$ (Figure 4b). The integrated heat release remains relatively constant at $Q = 1300 \pm 400 \text{ J g}^{-1}$ as a function of both the heating rate and the mass (Figure 5). A plot of $\ln(f(\alpha))$ versus α exhibits a concave downward shape (Figure 6).

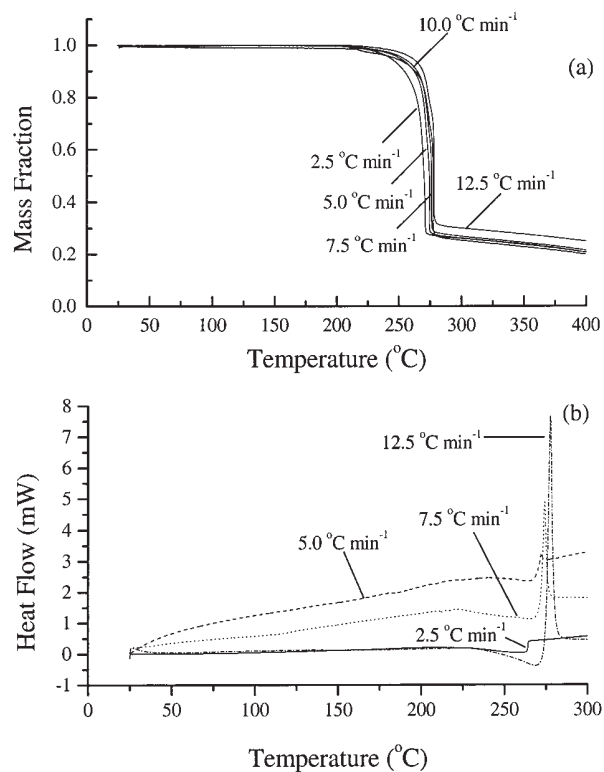


Figure 3. (a) Pierced pan nonisothermal TGA traces of NTO samples acquired at various constant heating rates. (b) Pierced pan nonisothermal DSC traces for NTO samples collected at constant heating rates.

Discussion

Open Pan Samples. The mass loss in Figure 1a occurring below the melting point for lower heating rates is suggestive of sublimation. However, the multistage nature of the mass loss in the TGA traces shows that more than simple sublimation occurs in an open pan. The change in the slope and shape of the initial mass loss with heating rate likely contributes to the sharp rise and fall in E_{α} for $0.0 < \alpha < 0.1$ (Figure 2a). The shallow decrease from $E_{\alpha} = 155 \text{ kJ mol}^{-1}$ at $\alpha = 0.1$ to $E_{\alpha} = 115 \text{ kJ mol}^{-1}$ at $\alpha = 1.0$ is similar to and overlaps with WB's recommended range for NTO sublimation of $E_A = 108\text{--}130 \text{ kJ mol}^{-1}$. The broad endotherm in the DSC trace of Figure 1b that occurs below the melting point of NTO is also characteristic of sublimation. The early portion of this broad endotherm shows much less temperature sensitivity than the sharper structured feature that appears at the latter stages of the endotherm. Thus, the shape of the endotherm can account for the increase in E_{α} over $0 < \alpha < 0.33$. Isoconversional analysis of the later, more temperature dependent region of the endotherm yields activation energies that slowly increase from $E_{\alpha} = 115 \text{ kJ mol}^{-1}$ to $E_{\alpha} = 130 \text{ kJ mol}^{-1}$ for $0.33 < \alpha < 0.95$ that are in agreement with WB's recommended values for sublimation.

Pierced Pan Samples. Compared to open pan samples, nonisothermal TGA traces change considerably when collected in a pierced pan (Figure 3a). First, the temperature range of the mass loss shifts to higher temperatures and occurs largely above the melting point. Such behavior is consistent with sublimation dominating in an open pan and thermal decomposition dominating in a pierced pan. Second, the mass loss occurs in a single stage, which suggests that a single process occurs under these conditions. Third, the stronger temperature dependence in pierced pan experiments indicates a larger activation energy for the condensed-phase process than that for sublimation in an open

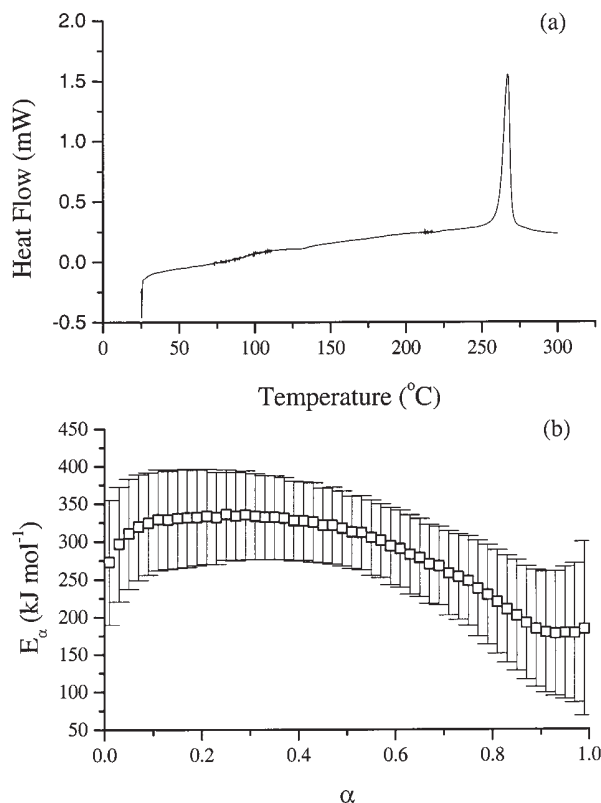


Figure 4. (a) A nonisothermal DSC trace acquired at $\beta = 5.0 \text{ }^\circ\text{C min}^{-1}$ for a closed pan sample of NTO. (b) E_α as a function of α created from the application of isoconversional analysis to nonisothermal DSC curves collected at $\beta = 1.0, 2.5, 5.0, 7.5, 10.0, 12.5,$ and $15.0 \text{ }^\circ\text{C min}^{-1}$ for closed pan samples of NTO.

pan. Fourth, only 78% of the initial mass is lost in pierced pan experiments compared to mass loss that approaches 100% in open pan experiments. The remaining mass in pierced pan experiments is consistent with previous reports of the formation of a solid residue during the thermal decomposition of NTO between 220 and 350 $^\circ\text{C}$.^{8,10,13,14,27–29} Probing by IR in the rapid heating of NTO ($\beta = 150\text{--}300 \text{ }^\circ\text{C min}^{-1}$), Brill et. al. observed the formation of gaseous decomposition products and a residue attributed to a melon-like, cyclic azine polymer that consists of $\leq 20\%$ of the initial mass,²⁹ in accord with our pierced pan TGA results. A simultaneous thermogravimetric modulated beam mass spectrometry (STMBMS) study supports competitive sublimation and condensed-phase thermal decomposition of NTO. The thermal decomposition leads to the formation of gaseous products and a solid residue believed to be polyurea- and polycarbamate-like in nature.¹³

A competition between sublimation and exothermic condensed-phase decomposition of NTO in this work is exhibited in the pierced pan DSC traces in Figure 3b. At a heating rate of $\beta = 2.5 \text{ }^\circ\text{C min}^{-1}$, only a broad endotherm suggestive of sublimation appears. At $\beta = 5.0 \text{ }^\circ\text{C min}^{-1}$, a small exotherm succeeds the broad endotherm. This exotherm increases in size with increasing heating rate. Hence, condensed-phase exothermic decomposition becomes increasingly important relative to sublimation with increasing β in pierced pan samples. A positive initial slope in a plot of the heat release versus β shows that the dominant process at higher heating rates, exothermic decomposition, has a higher activation energy than the dominant process at lower heating rates, sublimation (Figure 5a). A competition between vaporization and decomposition in the heating of RDX has been reported.²⁴ Vaporization was determined to have a lower E_α

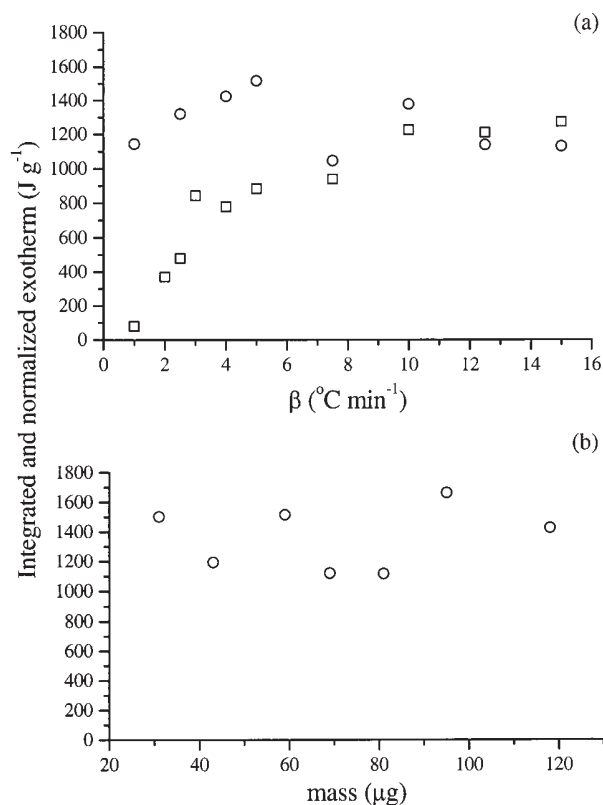


Figure 5. (a) Integrated and normalized heat release of the exotherm of nonisothermal DSC curves as a function of β for pierced pan (\square) and closed pan (\circ) samples of NTO. (b) Integrated and normalized heat release versus mass for nonisothermal DSC traces of closed pan (\circ) NTO samples.

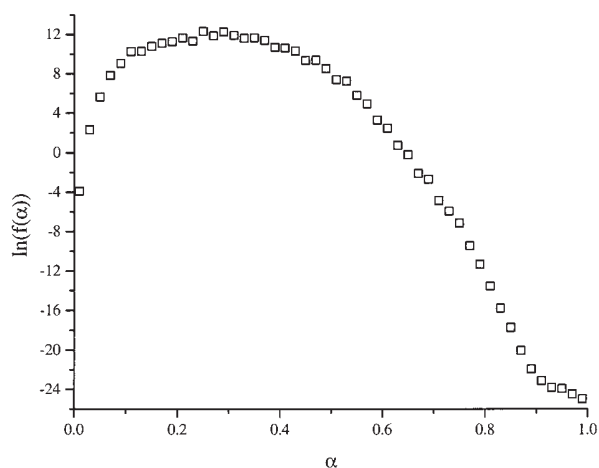


Figure 6. $\ln(f(\alpha))$ versus α obtained by reconstructing the empirical reaction model $f(\alpha)$. The product $Af(\alpha)$ versus α was determined using isoconversional analysis for which $\ln A = 58.1 \text{ s}^{-1}$ was calculated.

and to dominate at lower heating rates and decomposition to have a higher E_α and to dominate at higher heating rates. For the competitive processes observed in both the RDX and NTO systems, only a method of analysis such as the isoconversional method, which can determine the variation in E_α with α , can account for the relative contributions of each process and provide an adequate description of the global energetics in such systems.

Closed Pan Samples. Nonisothermal DSC traces for closed pan samples show only a sharp endotherm near the melting point for all heating rates studied (Figure 4a). A heat release of $Q = (1.3 \pm 0.4) \times 10^3 \text{ J g}^{-1}$ (169 kJ mol^{-1}) determined to be

independent of both β and the mass for closed pan samples is very similar to the asymptotic value of the heat release versus β in pierced pan experiments (Figure 5). This similarity suggests that the same process is dominant in pierced pan experiments at high heating rates and in closed pan experiments. This process is attributed to direct condensed-phase decomposition of NTO that generates gas-phase decomposition products (vide supra); its activation energy can be best determined in a closed pan experiment where sublimation is suppressed.

Isoconversional analysis of the exotherm in closed pan experiments yields activation energies that increase from 273 kJ mol⁻¹ at $\alpha = 0.01$ to a plateau of 333 kJ mol⁻¹ for $0.17 \leq \alpha \leq 0.35$ before decreasing to 184 kJ mol⁻¹ at $\alpha = 0.99$ (Figure 4b). This plateau falls within the range of 326–364 kJ mol⁻¹ that WB recommend for the thermal decomposition of NTO.¹¹ However, since the decomposition is autocatalytic,^{3,8,10,13,14} previous studies that have ascribed single values of the activation energy cannot accurately describe the entire decomposition. Only by using a tool such as isoconversional analysis to determine the functional dependence of E_α with α can both regions of NTO thermal decomposition be quantified. To our knowledge, the decrease in E_α with α after the plateau region to a final value of $E_\alpha = 184$ kJ mol⁻¹ marks the first quantitative description of the autocatalytic phase of the condensed-phase thermal decomposition of NTO. A decreasing E_α with α describes chemical autocatalysis in which the concentration of an intermediate that provides an alternative lower energy pathway builds up during the decomposition.²³ The observation of autocatalysis in both open^{8,13} and closed^{10,14,28,29} systems strongly implicates a solid-phase species such as a polymeric residue^{13,29} as an intermediate which enhances further decomposition.

Insight into the physical basis for autocatalysis in the latter stages of the thermal decomposition of NTO can be gained by using isoconversional analysis to reconstruct the reaction model, $f(\alpha)$. This methodology can determine both E_α and the product $Af(\alpha)$ as a function of α .²⁶ A fundamental assumption of this approach is that the α dependence of $Af(\alpha)$ is contained in $f(\alpha)$. A can be determined independent of $f(\alpha)$,²⁶ and for NTO, $\ln A = 58.1$ s⁻¹ has been calculated. This same method has computed $f(\alpha)$, and a plot of $\ln(f(\alpha))$ versus α exhibits a concave downward shape (Figure 6). Equation 1 shows that reporting A and the α dependence of both E_α and $f(\alpha)$ provides a comprehensive description of the decomposition kinetics of NTO. Furthermore, these three quantities are needed in to make kinetic predictions about the times to reach a particular extent of decomposition for either an isothermal or a nonisothermal heating program.

Conclusions

Nonisothermal TGA and DSC have shown sublimation and condensed-phase exothermic decomposition to be competitive during the heating of NTO. Sublimation occurs most readily in an open pan. Both sublimation and exothermic decomposition take place in the semiconfined environment of pierced pan samples; sublimation occurs more readily at lower heating rates, and exothermic decomposition dominates at higher heating rates. The competition between these two processes is apparent from a shift in the mass loss to temperatures above the melting point and from a change to single-stage mass loss in pierced pan TGA experiments compared to those performed in open pans. Further, an increase in the heat release as a function of heating rate in pierced pan DSC experiments shows that condensed-phase decomposition is favored at higher heating rates and that it has a larger activation energy than sublimation. An activation energy

for exothermic condensed-phase decomposition of NTO of 333 kJ mol⁻¹ for $0.17 \leq \alpha \leq 0.35$ and a decrease during the autocatalytic period to 184 kJ mol⁻¹ at $\alpha = 0.99$ were determined by isoconversional analysis of closed pan DSC experiments. Thus, the autocatalytic phase of NTO decomposition has been quantified for the first time. Under closed pan conditions, a rather constant heat flow of $Q = (1.3 \pm 0.4) \times 10^3$ J g⁻¹ (169 kJ mol⁻¹) is observed that is independent of both β and the mass. By quantifying all three processes in its activation, sublimation, decomposition, and autocatalysis, this work has provided a more detailed understanding of the thermal stability of NTO.

Acknowledgment. We thank Mettler-Toledo, Inc. for the generous donation of the TGA and DSC instruments used in this study. Partial support for this work from the Ballistic Missile Defense Organization and the Office of Naval Research under MURI Contract No. N00014-95-1-1339 and from the University of Utah Center for Simulation of Accidental Fires and Explosions (Department of Energy, Lawrence Livermore National Laboratory Subcontract B341493) is gratefully acknowledged.

References and Notes

- (1) Lee, K.-Y.; Chapman, L. B.; Coburn, M. D. *J. Energ. Mater.* **1987**, *5*, 27.
- (2) Spear, R. J.; Louey, C. N.; Wolfson, M. G. NTIS Report (MRL-TR-89-18, DODA-AR-005-708; Order No. AD-A215063), 39 pp. Gov. Rep. Announce. Index (U.S.): 1990, 90(7), Abstr. No. 015,731.
- (3) Prabhakaran, K. V.; Naidu, S. R.; Kurian, E. M. *Thermochim. Acta* **1994**, *241*, 199.
- (4) Hara, Y.; Taniguchi, H.; Ikeda, Y.; Takayama, S.; Nakamura, H. *Kayaku Gakkaishi* **1994**, *55*, 183.
- (5) Yi, X.; Rongzu, H.; Xiyu, W.; Xiayun, F.; Chunhua, Z. *Thermochim. Acta* **1991**, *189*, 283.
- (6) Yi, X.; Rongzu, H.; Chaoqing, Y.; Guofu, F.; Jihua, Z. *Propellants, Explos., Pyrotech.* **1992**, *17*, 298.
- (7) Ostmark, H.; Bergman, H.; Aqvist, G.; Langlet, A.; Persson, B. *Proceedings of the 16th International Pyrotechnics Seminar*, Jonkoping, Sweden, June 1991; Royal Swedish Academy of Sciences: Stockholm, 1991; p 874.
- (8) Menapace, J. A.; Marlin, J. E.; Bruss, D. R.; Dascher, R. V. *J. Phys. Chem.* **1991**, *95*, 5509.
- (9) Oxley, J. C.; Zhou, Z.; Smith, J. L.; McKenney, R. L. *Proceedings of the International American Defense Preparedness Association Symposium on Energetic Materials Technology*, March 1994; American Defense Preparedness Association: Orlando, Florida, 1994; p 155.
- (10) Oxley, J. C.; Smith, J. L.; Zhou, Z.; McKenney, R. L. *J. Phys. Chem.* **1995**, *99*, 10383.
- (11) Williams, G. K.; Brill, T. B. *J. Phys. Chem.* **1995**, *99*, 12536.
- (12) Brill, T. B.; Gongwer, P. E.; Williams, G. K. *J. Phys. Chem.* **1994**, *98*, 12242.
- (13) Minier, L.; Behrens, R.; Burke, T. J. *33rd JANNAF Combustion Subcommittee Meeting*, Monterey, CA, 1996; CPIA Publication #653, Vol. 2; Chemical Propulsion Information Agency: Baltimore, Maryland, 1996; p 427.
- (14) Oxley, J. C.; Smith, J. L.; Rogers, E.; Dong, X. X. *J. Phys. Chem. A* **1997**, *101*, 3531.
- (15) Vyazovkin, S.; Wight, C. A. *Annu. Rev. Phys. Chem.* **1997**, *48*, 125.
- (16) Vyazovkin, S. *J. Comput. Chem.* **1997**, *18*, 393.
- (17) Vyazovkin, S. *J. Comput. Chem.* **2001**, *22*, 178.
- (18) Galwey, A. K.; Brown, M. E. *Thermal Decomposition of Ionic Solids*; Elsevier: Amsterdam, 1999.
- (19) Vyazovkin, S.; Wight, C. A. *Chem. Mater.* **1999**, *11*, 3386.
- (20) Vyazovkin, S.; Wight, C. A. *Anal. Chem.* **2000**, *72*, 3171.
- (21) Vyazovkin, S.; Wight, C. A. *J. Phys. Chem. A* **1997**, *101*, 5653.
- (22) Vyazovkin, S.; Wight, C. A. *J. Phys. Chem. A* **1997**, *101*, 7217.
- (23) Lofy, P. M.S. Thesis, University of Utah, Salt Lake City, UT, 1999.
- (24) Long, G. T.; Vyazovkin, S.; Brems, B. A.; Wight, C. A. *J. Phys. Chem. B* **2000**, *104*, 2570.
- (25) Vyazovkin, S.; Wight, C. A. *J. Phys. Chem. A* **1997**, *101*, 8279.
- (26) Long, G. T.; Wight, C. A. Submitted to *J. Phys. Chem. B*.
- (27) Beard, B. C.; Sharma, J. *J. Energ. Mater.* **1989**, *7*, 181.
- (28) Rothgery, E. F.; Audette, D. E.; Wedlich, R. C.; Csejka, D. A. *Thermochim. Acta* **1991**, *185*, 235.
- (29) Williams, G. K.; Palopoli, S. F.; Brill, T. B. *Combust. Flame* **1994**, *98*, 197.